Hole-Growth Instability in the Dewetting of Evaporating Polymer Solution Films*,†

X. GU[1,2], D. RAGHAVAN[1], J. F. DOUGLAS[3], A. KARIM[3]

[1] Polymer Program, Department of Chemistry, Howard University, 525 College Street, Northwest, Washington, D.C. 20059

[2] MS8615, Building Materials Division, National Institute of Standards and Technology, Gaithersburg, Maryland 20899

[3] MS8542, Polymers Division, National Institute of Standards and Technology, Gaithersburg, Maryland 20899

Received 11 June 2002; revised 1 October 2002; accepted 1 October 2002

ABSTRACT: We investigate the dewetting of aqueous, evaporating polymer [poly(acrylic acid)] solutions cast on glassy hydrophobic (polystyrene) substrates. As in ordinary dewetting, the evaporating films initially break up through the nucleation of holes that perforate the film, but the rapidly growing holes become unstable and form nonequilibrium patterns resembling fingering patterns that arise when injecting air into a liquid between two closely spaced plates (Hele–Shaw patterns). This is natural because the formation of holes in thin films is similar to air injection into a polymer film where the thermodynamic driving force of dewetting is the analogue of the applied pressure in the flow measurement. The patterns formed in the rapidly dewetting and evaporating polymer films become frozen into a stable glassy state after most of the solvent (water) has evaporated, leaving stationary patterns that can be examined by atomic force microscopy and optical microscopy. Similar patterns have been observed in water films evaporating from mica substrates, block copolymer films, and modest hole fingering has also been found in the dewetting of dry polymer films. From these varied observations, we expect this dewetting-induced fingering instability to occur generally when the dewetting rate and film viscosity are sufficiently large. © 2002 Wiley Periodicals, Inc. J Polym Sci Part B: Polym Phys 40: 2825–2832, 2002

Keywords: dewetting; Hele–Shaw flow cell; instability; fingering patterns; atomic force microscopy (AFM); spin coating

INTRODUCTION

The stability of polymer films against dewetting is of considerable technological and scientific importance because of their widespread use as photoresists, adhesives, lubricants, and paints.[1–3] These applications often require film homogeneity, uniform thickness, and durability. A single layer of polymer film is applied on a solid substrate in many applications (e.g., lubricants on magnetic disks), whereas for others (e.g., paints and gas-barrier coatings), several polymer layers (e.g., top coat and primer) are successively applied by evaporating the solvent from a polymer solution.

The evaporation of solvent from polymer films can have a large influence on the resulting film morphology. In blend films, the evaporation process can lead to significant changes in blend mis-

*Contribution from the March 2002 Meeting of the American Physical Society—Division of Polymer Physics, Indianapolis, Indiana

†Certain commercial instruments and materials are identified in this article to adequately describe the procedure. In no case does such identification imply recommendation or endorsement by the National Institute of Standards and Technology, nor does it imply that the instruments or materials are necessarily the best available for the purpose

Correspondence to: D. Raghavan (E-mail: draghavan@howard.edu)

Journal of Polymer Science: Part B: Polymer Physics, Vol. 40, 2825–2832 (2002)

cibility, resulting in phase separation within the film and pattern formation associated with the surface-tension differences between the polymer components that cause the surface of the film to buckle in response to the phase separation within the film.[4–6] Convective flows within evaporating polymer solutions can lead to a Marangoni pattern formation that can have a large influence on film roughness in the resulting dried glassy or entangled polymer films.[7] Evaporation can also lead to dewetting (hole formation and film breakup into droplets) in films that would be thermodynamically stable under saturated vapor conditions[8–11] so that film stability can be influenced by controlling the rate of evaporation.

Although there have been numerous studies of the dewetting of uniform polymer films spun-cast on nearly homogeneous substrates,[12–23] the investigation of films that dewet in the course of drying is limited. Previous studies on evaporating water films on mica substrates indicate the formation of holes as in ordinary dewetting, but the boundary of the rapidly growing holes breaks up into fingering patterns that resemble nonequilibrium crystallization patterns[8–12] and Hele–Shaw flow patterns[24,25]. (an example of the Hele–Shaw pattern formation is considered subsequently). In this article, we show that similar nonequilibrium growth patterns are exhibited in evaporating polymer solution films dewetting from the substrate on which they are cast. We specifically consider the dewetting of a thin hydrophilic polymer [poly(acrylic acid) (PAA)] solution film cast on a hydrophobic [polystyrene (PS) film] substrate. We characterize the morphology of the resulting dewetted film by atomic force microscopy (AFM). To establish that the top layer in the dewetted polymer film is the PAA component and that the underlayer is the PS component, water was used to dissolve the top layer while keeping the PS underlayer intact. Fingering patterns have been observed in rapidly evaporating water films,[11] and our work demonstrates that a similar phenomenon arises in cast polymer films where the structure becomes "frozen" in the course of solvent evaporation from the film. The dewetting process is too rapid to allow us to conduct a kinetic study of this pattern formation.

EXPERIMENTAL

The hydrophobic substrates were prepared by spin-casting PS [Acros Organics, mass-average molecular mass (M_w): 250,000, glass-transition temperature (T_g): 104 °C] solution (toluene solvent) onto acetone-cleaned silicon wafers. An aqueous solution of PAA (Aldrich, M_w = 450,000, T_g = 106 °C) was then cast on these PS substrates. Air-drying of the PS films for 10 min was deemed adequate to remove most of the residual solvent from the PS coating. Although we did not anneal the samples, the films were quite glassy at room temperature; therefore, we expected residual solvent to have a minimal effect on our measurements. The PS substrate should be considered a solidlike, highly energetically unfavorable substrate for PAA whose topography can be manipulated by spin-casting conditions. The speed of spin-casting was maintained at 2000 rpm for 30 s. To minimize the effect of the silicon substrate on the dewetting morphologies, we considered a high PS concentration (8.0% mass fraction) and obtained thick PS films. Two different solution concentrations of PAA, 1.0 and 0.1% mass fraction, were used to vary the thickness of the PAA layer. Thickness of the cast films was measured by AFM. For this application, the film on the silicon was scratched with a knife to expose the bare silicon substrate. The average step height from the film surface to the surface of the substrate was used as an estimate of the film thickness. The thicknesses of the PAA films cast from 1.0 and 0.1% mass fraction solutions were 32 ± 2 and 10 ± 1 nm, respectively. The results reported here are the averages of three measurements.

The morphology and dewetting pattern of the cast films were imaged with a Dimension 3100 (Digital Instruments) scanning probe microscope in tapping mode under ambient conditions. Manufacturers' values for the tip radius and spring constant for the silicon cantilever probe were in the ranges of 5–10 nm and 20–100 N/m, respectively. Topographic and phase images were recorded simultaneously with a resonance frequency of approximately 300 kHz for the probe oscillation, a scan rate of 1 Hz, and a free-oscillation amplitude of 60 ± 5 nm. The measurements used a set-point ratio in the range of 0.6–0.8.

RESULTS AND DISCUSSION

Figure 1(A) portrays topographic (left) and phase (right) images of a PAA film cast on a PS substrate. The image (scan dimension, 2.5 × 2.5 μm)

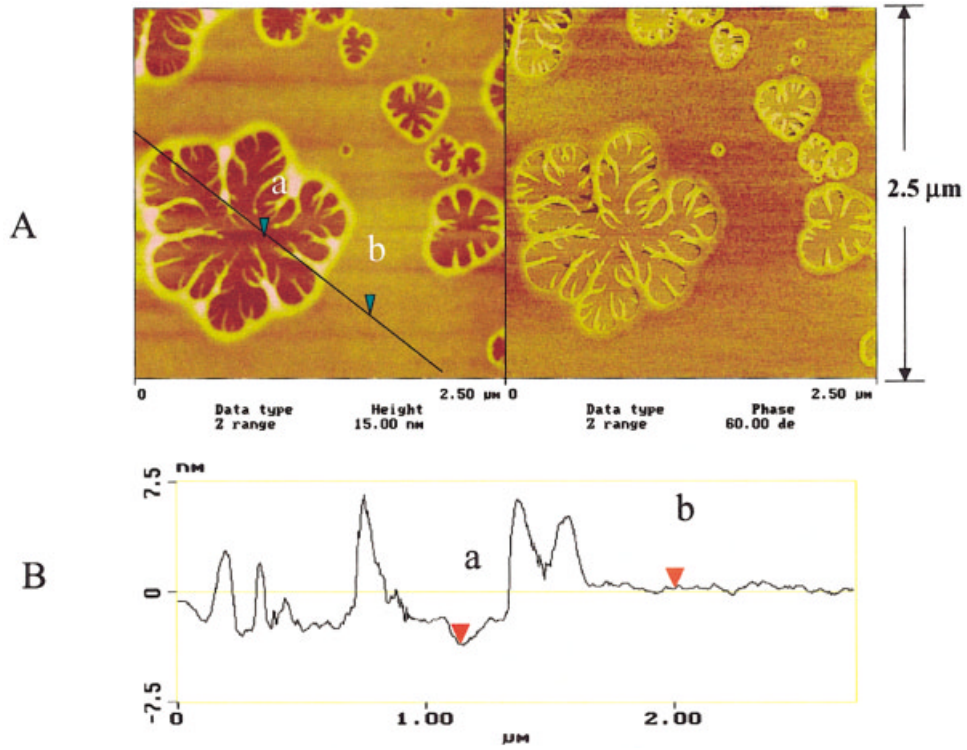

Figure 1. Tapping-mode AFM: (a) height and phase images of isolated fingering patterns and (b) line profile of height image for the PS/PAA film prepared by spin-coating 8.0 wt % PS in toluene and 0.1 wt % PAA in water. Color contrast from black to white represents a total range of 15 nm in the height image and 60° in the phase image. [Color figure can be viewed in the online issue, which is available at www.interscience.wiley.com.]

was obtained immediately after film casting and film drying, and the patterns apparently reveal no appreciable evolution of structure at later times. The sample in this figure was prepared by spin-casting 8.0% mass fraction PS in toluene on an acetone-cleaned silicon wafer with 0.1% mass fraction PAA for the top layer. We observe isolated "dense branching" or "seaweed" fingering patterns that are characteristic of a variety of nonequilibrium pattern-formation processes such as nonequilibrium crystal growth, growth of bacterial colonies, and fluid fingering in multiphase systems.[26–28] Note the tendency of the branches of the growing front to split as the pattern develops, which is a characteristic of seaweed growth. The size of the fingering pattern varies within the sample. The topographic image and its corresponding height profile [Fig. 1(B)] suggest that the interior region of the pattern is lower than the exterior flat region, whereas the fingers and the rim of the pattern are elevated.

In addition to the localized regions of dewetting in Figure 1, we occasionally observed patches in which the dewetting patterns impinge on each other. Figure 2 depicts topographic (left) and phase (right) images of another location of an as-prepared PS-PAA bilayer. Apparently, there are variations in the density of heterogeneities on the PS substrate that initiate film dewetting. Note the tendency of the dewetting patterns to deform when they strongly interact, another characteristic feature of this kind of nonequilibrium growth pattern as studied in the context of crystallization[29] and ordinary dewetting of uniform polymer films.[30] The interpretation of the pattern formation described previously requires that the elevated rims are PAA, whereas the depressions should reach down nearly to the PS substrate (a very thin layer of the dewetting fluid can sometimes remain on the "dry" regions). We attempted to identify the chemical nature of the "dry regions" by hydrolyzing the PAA layer and

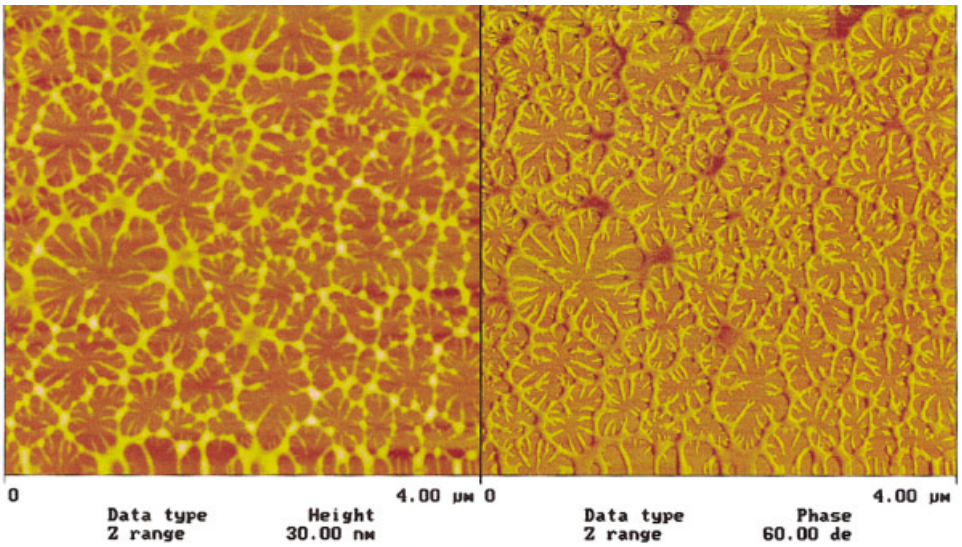

Figure 2. Tapping-mode AFM height and phase images of a cellular dewetting pattern on the PS/PAA film prepared by spin-coating 8.0 wt % PS in toluene and 0.1 wt % PAA in water. Color contrast from black to white represents a total range of 30 nm in the height image and 60° in the phase image. [Color figure can be viewed in the online issue, which is available at www.interscience.wiley.com.]

examining the change in the phase contrast by AFM measurements.[31] The contrast of the dewetted region increased with an increase in relative humidity (RH) suggesting residual PAA, but it is difficult to interpret this contrast change because of the many factors involved such as adhesion, mechanical properties, surface topography, and so forth.[32–40] During the humidity exposure study, the dewetting structure remained stable up to 90% RH, thereby suggesting limited mobility of the PAA chains. Although at >90% RH, the mobility of the PAA apparently became large enough for the PS layer to become exposed (as evidenced by a drop in the frictional force of the depressed regions). These results support our interpretation that the elevated dewetted regions are PAA and that the dewetted regions extend down close to the PS substrate.

The patterns in Figures 1 and 2 have a strong resemblance to water-film evaporation patterns,[9,10] but the polymer-film patterns become "frozen" in form once the film has dried sufficiently. This greatly facilitates the investigation of the patterns by AFM and other microscopy methods, but kinetic studies are not readily performed because of the rapid nature of the pattern formation. Previous work has emphasized that there is a similarity of this kind of pattern formation to nonequilibrium crystallization growth patterns[12,41] where seaweed patterns have been observed, but here we draw analogy to the problem of viscous fingering where we think there is a closer physical relation to our observations.

Seaweed growth patterns are characteristically found when a low-viscosity fluid is injected into a high-viscosity medium. Disorder (heterogeneity) tends to enhance the branching of such fingers.[39] A filmlike geometry exists when the viscous fluid is confined between two plates with a narrow gap between them. To make our comparison concrete, we demonstrate in Figure 3 an optical micrograph of Hele–Shaw patterns[25,42] generated by injecting air into deionized water confined between glass plates having a 50 μm separation. The field of view corresponds to 9.9 $\times$ 8.3 cm, resulting in large patterns. Successive contours indicate the position of the air–water front as it spreads into the water matrix. Initially the air boundary has a round shape governed by surface tension, but the moving front breaks up into fingers that split as they grow to form a branched viscous fingering pattern. The fingering instability in thin evaporating films has been described by Iyushnin et al.[10] who also emphasize the similarity of the fingering instability to a Rayleigh instability of a fluid thread corresponding to

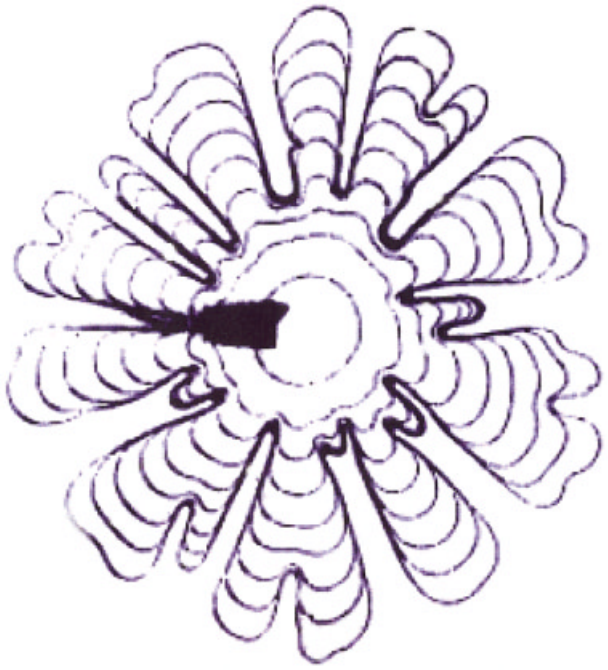

Figure 3. Hele–Shaw pattern formation for air injected into deionized water confined between glass plates. The temperature is 21 ° C, and the air pressure of the injected air is 14.3 kPa. Image dimension is 9.9 × 8.3 cm. The image is blurry because of the difficulty in achieving contrast in the measurements (these are new measurements provided for us by R. Ennis and P. Palffy-Muhoray of Kent State University). [Color figure can be viewed in the online issue, which is available at www.interscience.wiley.com.]

the rim of the growing dewetting hole. We include Figure 3 as a point of reference in our discussion of dewetting.

Next, we summarize our interpretation of dewetting in evaporating polymer solution films as a closely analogous process. Holes are formed in the PAA layer by nucleation (homogeneous nucleation from surface undulation and heterogeneous nucleation from impurities in the film and on the PS substrate), and these holes are normally circular in the early stages of dewetting. The initial formation of holes in thin film is similar to the injection of air into a highly viscous fluid confined to near two dimensions. At a late stage of dewetting, there is a strong tendency for the holes to coalesce, and this coalescence process largely determines the morphology of the late-stage dewetting pattern.[43] When the rims of growing holes eventually contact each other, the opposing faces flatten out because of increased viscous resistance encountered by the polymer, and a thin liquid ribbon is formed between neighboring holes by a merger of these rims. In late-stage dewetting, the branches grow from the rim by consecutive splitting of the leading tips as they grow away from the center of the pattern. Small droplets are visible on the tips of some branches in Figure 1(A), especially in the phase image. These droplets represent the termination points of the viscous fingers. This observation is consistent with other studies for high-molecular-weight PS on nonwetting substrates, which have shown that fingers develop from the rim and grow radially, and the fingers eventually pinch off leaving a trail of drops from the resulting Rayleigh instability.[44,45] Late-stage dewetting of PAA on PS film was reached while the solvent was evaporating from the spun-cast film. This is supported by observation of similar dewetting patterns when the sample was either annealed at 100 °C for 4 h or under ambient conditions for 24 h (the results are not shown). Because PAA has a T_g of 106 °C and is glassy when it is dry at ambient temperature, the growth of the fingers becomes frozen when the solvent (water) has sufficiently evaporated. Similarly, the role of external humidity on the film dewetting structure was noticed for volatile spin-coated dewetting collagen solution films,[39] where the balance between the dewetting process (heterogeneous nucleation or spinodal dewetting) and film thinning because of solvent evaporation strongly influences the dewetting morphology.

AFM images of thicker films made from 1.0% mass fraction PAA solutions cast on PS lead to patterns of even greater complexity, as illustrated in Figure 4. A dust particle in the center of the pattern serves as the nuclei for the dewetting process, resulting in a height variation in the radial direction. Compared with the fingering structure of the thin film (0.1% mass fraction PAA spun-cast on PS) shown in Figure 1, this isolated dewetting pattern has greater branching density. With an increase in the viscosity of the evaporating concentrated PAA solution, the velocity of hole growth is much slower, but the mismatch between the fluid viscosity of the film and the growing holes enhances the instability responsible for the flow pattern, again as in the Hele–Shaw measurements. The highly branched nature of the growth patterns is particularly striking in thick films and highly viscous casting solutions where the resulting viscous fingers be-

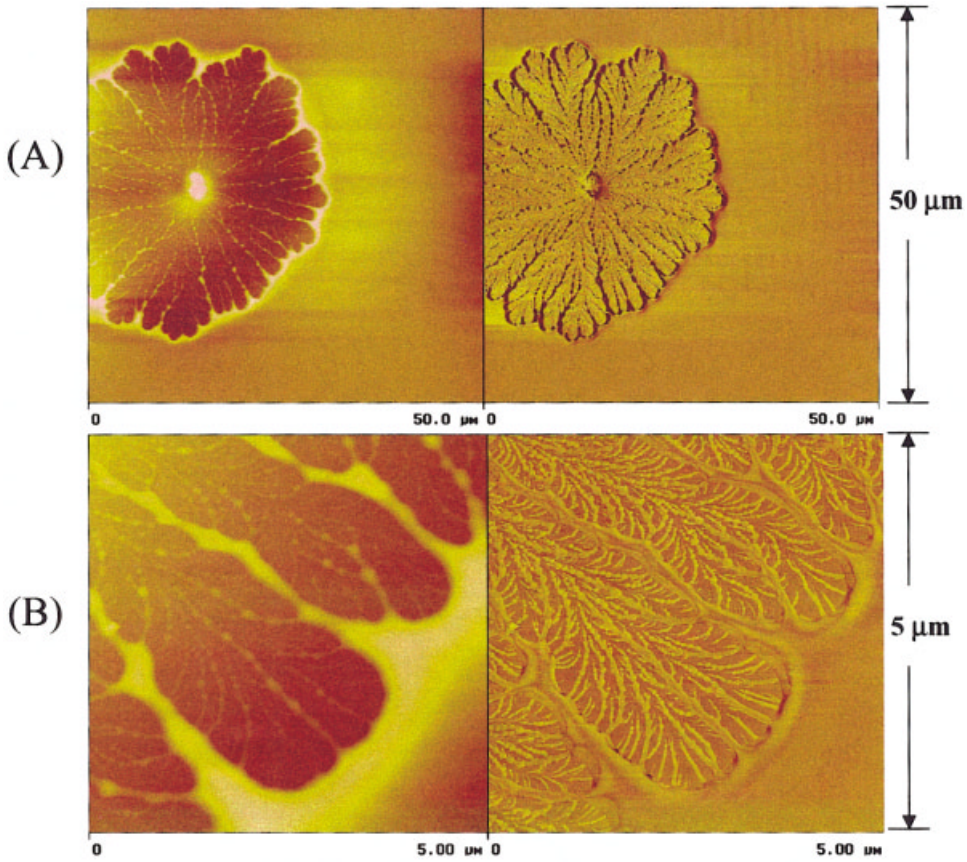

Figure 4. (a) A circular dewetting pattern centered at a defect (50 ×50 μm) and (b) dendritic growth pattern at high magnification (5 × 5 μm). Film was prepared by spin-coating 8.0% PS in toluene and 1.0 wt % PAA in water. Color contrast from black to white represents a total range of 250 nm in the height image (left) and 90° in the phase image (right) for both (a) and (b). [Color figure can be viewed in the online issue, which is available at www.interscience.wiley.com.]

come fractal objects. Fractal patterns having a similar fractal dimension to diffusion-limited aggregation have been shown to occur in Hele–Shaw pattern formation when the fluid spreads into a porous (i.e., heterogeneous) medium.[46–48] The branching structure of the pattern is characteristically influenced by the viscoelasticity of the fluid in the Hele–Shaw flows,[49,50] and the same is likely true for pattern formation in evaporating polymer solution films. Figure 4(b) depicts an AFM image of a fractal dewetting pattern at high magnification.

Similar fractal topographical patterns in thin films have been seen in block copolymer films[51] where dust particles seem to nucleate the patterns. Jagged dewetting holes forming in initially smooth polymer spun-cast films (little solvent evaporation occurs in the dewetting process in this case) have been attributed by Reiter[30] to the instability of the hole rim; therefore, this type of instability is not limited to evaporating films. Our results for evaporating polymer solution films and the suggested analogy with Hele–Shaw flows suggest that this type of flow instability should be general for rapidly dewetting viscous films. Rapid evaporating polymer films are particularly favorable for observing such patterns because dewetting tends to occur in relatively thick films, and hole-growth formation is often rapid.

The authors thank R. Ennis and P. Palffy-Muhoray of Kent State University for providing the image of the Hele–Shaw pattern shown in Figure 3. This work was supported by Air Force Office of Scientific Research.

REFERENCES AND NOTES

1. Wicks, Z. W.; Jones, F. N.; Pappas, S. P. In Organic Coatings: Science and Technology; Wiley-Interscience: New York, 1992.
2. Garbassi, F.; Morra, M.; Occhiello, E. In Polymer Surfaces; Wiley: Chichester, England, 1994.
3. Kheshgi, H. S.; Scriven, L. E. Chem Eng Sci 1991, 46, 519–526.
4. Sung, L.; Karim, A.; Douglas, J. F.; Han, C. C. Phys Rev Lett 1996, 76, 4368–4371.
5. Ermi, B. D.; Karim, A.; Douglas, J. F. J Polym Sci Part B: Polym Phys 1998, 36, 191–200.
6. Karim, A.; Slawecki, T. M.; Kumar, S. K.; Douglas, J. F.; Satija, S, K.; Han, C. C.; Russell, T. P.; Liu, Y.; Overney, R.; Sokolov, J.; Rafailovich, M. H. Macromolecules 1998, 31, 857–862.
7. Strawhecker, K. E.; Kumar, S. K.; Douglas, J. F.; Karim, A. Macromolecules 2001, 34, 4669–4672.
8. Elbaum, M.; Lipson, S. G. Phys Rev Lett 1994, 72, 3562–3565.
9. Elbaum, M.; Lipson, S. G.; Wettlaufer, J. S. Europhys Lett 1995*,* 29*,* 457–462.
10. Lyushnin, A. Y.; Golovin, A. V.; Pismen, L. M. Phys Rev E: Stat Phys Plasmas Fluids Relat Interdiscip Top 2002, 65, 021602.
11. Samid-Merzel, N.; Lipson, S. G.; Tannhauser, D. S. Phys Rev E: Stat Phys Plasmas Fluids Relat Interdiscip Top 1998, 57, 2906–2913.
12. Brener, E.; Muller-Krumbhaar, H.; Temkin, D.; Abel, T. Solid State Ionics 2000, 131, 23–33.
13. Melo, F.; Joanny, J. F.; Fauve, S. Phys Rev Lett 1989, 63, 1958–1961.
14. Limary, R.; Green, P. F. Langmuir 1999, 15, 5617–5622.
15. Limary, R.; Green, P. F. Macromolecules 1999, 32, 8167–8172.
16. Reiter, G.; Auroy, P.; Auvray, L. Macromolecules 1996, 29, 2150–2157.
17. Hamley, I. W.; Hiscutt, E. L.; Yang, Y. W.; Booth, C. J Colloid Interface Sci 1999, 209, 255–260.
18. Reiter, G. Phys Rev Lett 2001, 87, 166103-1–166103-4.
19. Masson, J.; Olufokunbi, O.; Green, P. F. Macromolecules 2002, 35, 6992–6996.
20. Limary, R.; Green, P. F. Macromolecules 2002, 35, 6486–6489.
21. Masson, J. L.; Green, P. F. J Chem Phys 2000, 112, 349–355.
22. Sferrazza, M.; Heppenstall-Butler, M.; Cubitt, R.; Bucknall, D.; Webster, J.; Jones, R. A. L. Phys Rev Lett 1998, 81, 5173–5176.
23. Higgins, A. M.; Sferrazza, M.; Jones, R. A. L.; Jukes, P. C.; Sharp, J. S.; Dryden, L. E.; Webster, J. Europhys J 2002, 8, 137–143.
24. Patterson, L. J Fluid Mech 1981, 113, 513–529.
25. McCloud, K. V.; Maher, J. V. Phys Rep 1995, 260, 139–185.
26. Ben-Jacob, E.; Garik, P. Nature 1990*,* 343*,* 523–530.
27. Ben-Jacob, E.; Shmueli, H.; Shochet, O.; Tenenbaum, A. Phys A 1992*,* 187*,* 378–424.
28. Ihle, T.; Müller-Krumbhaar, H. Phys Rev E: Stat Phys Plasmas Fluids Relat Interdiscip Top 1994, 49, 2872–2991.
29. Aboav, D. A. Metallography 1970, 3, 383.
30. Reiter, G. Langmuir 1993, 9, 1344–1351.
31. Gu, X.; Raghavan, D.; Douglas, J. F.; Karim, A. Unpublished data.
32. Raghavan, D.; Gu, X.; VanLandingham, M.; Nguyen, T.; Karim, A. Macromolecules 2000, 33, 2573–2583. We noticed a sharp increase in phase angle of the fingers with exposure to high relative humidity.[31] In general, the interpretation of phase-image contrast is rather complex, and we do not fully understand how to interpret the images. Several factors including surface mechanical properties,[32,33] surface topography,[34] interactions between tips and samples,[35,36] and capillary forces because of water layer on the tip and/or sample surface[34,37,38] can affect the contrast obtained by phase imaging.
33. Tamayo, J.; Garcia, R. Langmuir 1996, 12, 4430–4435.
34. Magonov, S. N.; Ellings, V.; Whangbo, M. H. Surf Sci 1997, 375, L385–L391.
35. Schmitz, I.; Schreiner, M.; Friedbacher, G.; Grasserbauer, M. Appl Surf Sci 1997, 115, 190–198.
36. Finot, M. O.; McDermott, M. T. J Am Chem Soc 1997, 119, 8564–8565.
37. Noy, A.; Sanders, C. H.; Vezenov, D. V.; Wong, S. S.; Leiber, C. M. Langmuir 1998, 14, 1508–1511.
38. Binggeli, M.; Mate, C. M. Appl Phys Lett 1994, 65, 415–417.
39. Maloy, K. J.; Feder, J.; Jossang, T. Phys Rev Lett 1985, 55, 2688–2691.
40. Han, T.; Williams, J. M.; BeeBe, T. P. Anal Chim Acta 1995, 307, 365–376.
41. Ferreiro, V.; Douglas, J. F.; Warren, J. A.; Karim, A. Phys Rev E: Stat Phys Plasmas Fluids Relat Interdiscip Top 2002, 65, art no. 051606.
42. Daccord, G.; Nittmann, J.; Stanley, H. E. Phys Rev Lett 1986, 56, 336–339.

43. Barnes, K. A.; Douglas, J. F.; Liu, D.; Bauer, B.; Amis, E. J.; Karim, A. Polym Int 2000, 49, 463–468.
44. Reiter, G. Phys Rev Lett 1992, 68, 75–78.
45. Thiele, U.; Mertig, M.; Pompe, W. Phys Rev Lett 1998, 80, 2869–2872.
46. Arnéodo, A.; Couder, Y.; Grasseau, G.; Hakim, Y.; Rabaud, M. Phys Rev Lett 1989, 63, 984–987.
47. Tang, C. Phys Rev A: At Mol Opt Phys 1985, 31, 1977–1979.
48. Paterson, L. Phys Rev Lett 1984, 52, 1621–1624.
49. Buka, A.; Kertész, J.; Vicsek, T. Nature 1986, 323, 424–425.
50. Zhao, H.; Maher, J. V. Phys Rev E: Stat Phys Plasmas Fluids Relat Interdiscip Top 1993, 47, 4278–4283.
51. Koneripalli, N.; Bates, F. S.; Fredrickson, G. H. Phys Rev Lett 1998, 81, 1861–1864.